

See discussions, stats, and author profiles for this publication at: <https://www.researchgate.net/publication/231242637>

# Mechanism of Calcium Oxalate Monohydrate Kidney Stones Formation: Layered Spherulitic Growth

ARTICLE *in* CHEMISTRY OF MATERIALS · JANUARY 2010

Impact Factor: 8.35 · DOI: 10.1021/cm901751g

---

CITATIONS

13

---

READS

127

## 7 AUTHORS, INCLUDING:



Alexei A Bokov

Simon Fraser University

116 PUBLICATIONS 2,794 CITATIONS

[SEE PROFILE](#)



Byron D Gates

Simon Fraser University

108 PUBLICATIONS 8,982 CITATIONS

[SEE PROFILE](#)

## Mechanism of Calcium Oxalate Monohydrate Kidney Stones Formation: Layered Spherulitic Growth

Usama Al-Atar,<sup>†</sup> Alexei A. Bokov,<sup>†</sup> Dan Marshall,<sup>‡</sup> Joel M. H. Teichman,<sup>§</sup>  
Byron D. Gates,<sup>†</sup> Zuo-Guang Ye,<sup>\*,†</sup> and Neil R. Branda<sup>\*,†</sup>

<sup>†</sup>4D LABS, Department of Chemistry, and <sup>‡</sup>Department of Earth Sciences, Simon Fraser University, Burnaby, British Columbia, Canada, and <sup>§</sup>Department of Urologic Sciences, University of British Columbia, Vancouver, British Columbia, Canada

Received June 23, 2009. Revised Manuscript Received October 16, 2009

The morphology of calcium oxalate monohydrate (COM) kidney stones is studied using polarized light microscopy and X-ray diffraction. We show that polycrystalline structure of COM stones exhibits spherulitic texture where the arrangement of crystallites indicates that their fast growth direction is perpendicular to the corresponding radius of spherulite, resulting in the layered morphology. This is in contrast to “normal” spherulites, where the crystal growth process leads to the formation of a radiating array of fiber crystallites. We demonstrate that COM stones consist of spherulitic domains. The domains have the shape of comparatively narrow randomly distorted cones in which the crystallites form strong texture, so that their crystallographic axes have almost the same directions and the [100] crystallographic planes are nearly perpendicular to the radial direction of the domain. However, the order among the domains does not exist. Deviations of their radial directions from the corresponding radial directions of the whole stone are not large as a rule, while the other crystallographic directions of the domains are randomly distributed. A model of layered spherulitic growth explaining the observed morphology is proposed. The model suggests that every domain is formed by means of a continuous crystallization process periodically inhibited by precipitation of organic material so that alternating organic and polycrystalline layers appear. Fine crystalline channels remaining in organic layers connect neighboring crystalline layers and maintain, thereby, the coherence of crystal structure all over the domain. Preformed COM microcrystals occasionally adsorbed from urine on the surface of the growing organic layer serve as seeds for new spherulitic domains. The results are important for understanding the general principles of biomineralization, and spherulitic crystallization and could lead to the development of new strategies for preventing kidney stone formation.

### 1. Introduction

Kidney stones are polycrystalline aggregates containing minerals of various compositions and small concentrations of organic compounds such as proteins or lipids embedded between the crystallites.<sup>1–3</sup> The stones are usually found attached to epithelial cells lining the renal tubules of the kidney and may reach the size of a few centimeters.

Calcium oxalate monohydrate (COM), also known as the mineral whewellite with the formula  $\text{CaC}_2\text{O}_4 \cdot \text{H}_2\text{O}$ , is the predominant and quite often the single crystalline component in the majority of kidney stones.<sup>4</sup> Interestingly, formation of calcium oxalate crystals is not limited to individuals who end up developing kidney stones, and several studies have confirmed the existence of calcium

oxalate crystals in urine of nonstone formers.<sup>5,6</sup> COM is also found in other materials of mineral and biological nature including plants (e.g., cacti),<sup>7</sup> hydrothermal deposits,<sup>8</sup> coal, and sedimentary nodules.<sup>9</sup> In many cases, it exists in the form of separate microcrystals instead of being combined into complex aggregates similar to kidney stones.

Stone development occurs in two steps: nucleation and growth. Currently, the general consensus is that calcium oxalate crystals in urine appear through a heterogeneous, not homogeneous, nucleation, where the numerous components found in various concentrations in the kidney make heterogeneous nucleation more likely.<sup>10</sup> Materials

\*To whom correspondence should be addressed. Phone: (778) 782-8061. Fax: (778) 782-3765. Email: zye@sfu.ca (Z.-G.Y.); nbranda@sfsu.ca (N.R.B.).  
(1) Stacholy, J.; Goldberg, E. P. *Scanning Electron Microsc.* **1985**, II, 781–787.  
(2) Khan, S. R.; Hackett, R. L. *J. Urol.* **1993**, 150, 239–245.  
(3) Leusmann, D. B. *Scanning Electron Microsc.* **1983**, 387–396.  
(4) Benramdane, L.; Bouatia, M.; Idrissi, M. O. B.; Draoui, M. *Spectrosc. Lett.* **2008**, 41, 72–80.

- (5) Robertson, W. G.; Peacock, M.; Nordin, B. E. C. *Lancet* **1969**, 25, 21–24.  
(6) Robertson, W. G. *Physical chemical aspects of calcium stone formation in the urinary tract*; Plenum Press: New York, 1976.  
(7) Hartl, W. P.; Klapper, H.; Barbier, B.; Ensikat, H. J.; Dronskowski, R.; Muller, P.; Ostendorp, G.; Tye, A.; Bauer, R.; Barthlott, W. *Can. J. Botany* **2007**, 85, 501–517.  
(8) Hoffmann, B. A.; Bernasconi, S. M. *Chem. Geol.* **1998**, 149, 127–146.  
(9) Žák, K.; Skála, R. *Chem. Geol.* **1993**, 106, 123–131.  
(10) Coe, F. L.; Favus, M. J.; Asplin, J. R. *Nephrolithiasis*. In *Brenner & Rector's The Kidney*, 7th ed.; Brenner, B. M., Ed. W. B. Saunders: Philadelphia, 2004; Vol. 2, pp 1819–1866.

acting as nidi for kidney stone growth remain unclear. It has been suggested that COM crystals deposition may occur on a preformed calcium phosphate nidus, known as Randall's plaques.<sup>11–13</sup> However, Randall's plaques are not found in all individuals suffering from kidney stones, such as intestinal bypass patients.<sup>14</sup> Furthermore, recent work on knockout mice demonstrates that the presence of calcium phosphate is not necessary for calcium oxalate crystal deposition.<sup>15</sup> Alternatively, the free and fixed particle theories suggest that calcium oxalate crystals can grow large enough to block the ducts of Bellini or adhere to the wall of the kidney and act as nidi for stone growth, respectively.<sup>16,17</sup> Of course, a combination of factors may be responsible for the initial development of these unwanted mineral aggregates.

Although extensive research has been conducted over the past century on the formation of kidney stones, the mechanism by which COM crystals grow into stones is poorly understood.<sup>18</sup> Some evidence suggests that micro-crystals preformed in urine deposit onto a surface of an existing stone, and its size increases thereby.<sup>19,20</sup> This mechanism gave rise to the notion that in order to have stone growth there must be adhesion between preformed crystals. The adhesion is thought to be provided by urinary proteins and other organic materials acting as glue.

Another probable mechanism is the direct crystal growth of the stone from a nucleolus, where adsorption of the molecules or ions of stone-forming compounds occurs one by one on the crystal surface while urine serves as their supersaturated solution (monoepitaxial growth). Heteroepitaxial growth, which refers to the direct growth of one crystal on a surface of different composition with a near exact fit between crystal lattices of the growing crystal and the substrate, can also be involved.<sup>21</sup> In such a way, the stones containing different crystalline compounds appear.

It is clear that the real process of kidney stone growth can hardly be directly observable. To model the kinetics, researchers try to grow the stone-forming crystals under conditions simulating the human kidney.<sup>22–25</sup> However, it is not easy to reproduce the conditions of stone formation. The other approach is to draw conclusions indirectly based on the morphology of real stones. In performing the latter method, it was noticed in particular that COM

kidney stones resemble so-called spherulites.<sup>3,26</sup> Spherulitic texture is observed in many natural and synthetic polycrystalline materials such as igneous rocks, high polymers, and metal inorganic salts.<sup>27,28</sup>

In this work, we utilize polarizing optical microscopy and X-ray diffraction (XRD) to study the morphology of COM kidney stones and to reveal possible mechanisms of their formation. The morphology appears to be quite complex because of the low (monoclinic) crystal symmetry of COM, the spherulitic arrangement of crystallites, and the significant role of foreign (organic) substances in the course of stone formation. However, we believe that the main features of the stone growth mechanism are revealed. This is important for the development of strategies for preventing kidney stone formation and is also helpful in understanding the general principles of spherulitic crystallization.

## 2. Experimental Procedures

**Materials.** Seven COM kidney stones were obtained from percutaneous nephrolithotomy cases, and their identity was confirmed in our laboratory using X-ray diffraction (XRD) by comparing their diffraction patterns to crystalline calcium oxalate monohydrate (99.9%) purchased from Fisher Scientific and calculations by means of the computer program LAZY PULVERIX.<sup>29</sup> The stones were stored at room temperature. Each stone was cut along a plane close to its middle using a razor blade, and the cut surface of one-half of each stone was polished and fixed onto a glass slide for the polarized optical microscopy studies. The surface of the other half of each stone was polished for further characterization using XRD.

**COM Crystals Synthesis.** All chemicals used for the COM crystallization experiments were purchased from Sigma-Aldrich. COM crystals were prepared as described in the literature by combining aqueous solutions of  $\text{CaCl}_2$  (10 mM) and sodium oxalate (10 mM  $\text{Na}_2\text{C}_2\text{O}_4$ ) at room temperature in an ionic buffer (150 mM NaCl and 10 mM HEPES (*N*-[2-hydroxy]-perazine-*N'*-[2-ethanesulfonic acid]) titrated to pH 7.5 with NaOH).<sup>30</sup>  $\text{CaCl}_2$  and  $\text{Na}_2\text{C}_2\text{O}_4$  were volumetrically added to the ionic buffer in a 10:1 ratio of calcium to oxalate, and the solutions were usually prepared in a total volume of 10 mL in a new glass vial with a 1 cm × 1 cm square glass piece on its base for crystals to settle on it. This ratio was chosen because it is known to yield the largest size of COM crystals.<sup>30</sup> After the addition of all components, the vials were shaken vigorously for approximately 15 s, and left to stand undisturbed at room temperature for 72 h. The crystals were collected by removing the square glass slide and washed with Millipore water to remove NaCl. The identity of the crystals was confirmed by X-ray diffractometry; their thickness was determined using an Alpha-Step IQ profiler (KLA Tencor, USA).

**COM Kidney Stones Cross Sections.** One of the halves of six of the kidney stones were polished by Vancouver Petrographics Ltd. (Langley, BC, Canada). Each sample was individually embedded in Petro-epoxy (refractive index of 1.54) and left to

- (11) Randall, A. *J. Urol.* **1940**, *44*, 580–589.
- (12) Matlaga, B. R.; Coe, F. L.; Evan, A. P.; Lingeman, J. E. *J. Urol.* **2007**, *177*, 31–38.
- (13) Evan, A. P.; Lingeman, J. E.; Coe, F. L.; Worcester, E. M. *Semin. Nephrol.* **2008**, *28*, 200–213.
- (14) Ryall, R. L. *Urol. Res.* **2008**, *36*, 77–97.
- (15) Khan, S. R.; Glenton, P. A. *Am. J. Physiol. Renal Physiol.* **2008**, *294*, F1109–F1115.
- (16) Finlayson, B.; Reid, F. *Invest. Urol.* **1978**, *15*, 442–448.
- (17) Kok, J.; Khan, S. R. *Kidney Int.* **1994**, *46*, 847–854.
- (18) Wesson, J. A.; Ward, M. D. *Elements* **2007**, *3*, 415–421.
- (19) Sandersius, S.; Rez, P. *Urol. Res.* **2007**, *35*, 287–293.
- (20) Saw, N. K.; Rao, P. N.; Kavanagh, J. P. *Urol. Res.* **2008**, *36*, 11–15.
- (21) Lonsdale, K. *Nature* **1968**, *217*, 56–58.
- (22) Finlayson, B. *Invest. Urol.* **1972**, *9*, 258–263.
- (23) Millan, A. *Cryst. Growth Des.* **2001**, *1*, 245–254.
- (24) Nancollas, G. H. *Proc. EDTA* **1983**, *20*, 386–397.
- (25) Miller, J. D.; Randolph, A. D.; Drach, G. W. *J. Urol.* **1977**, *117*, 342–345.

- (26) Sokol, E.; Nigmatulina, E.; Maksimova, N.; Ghiglntsev, A. *Eur. J. Mineral.* **2005**, *17*, 285–295.
- (27) Keith, H. D.; Padden, F. J., Jr. *J. Appl. Phys.* **1963**, *34*, 2409–2421.
- (28) Magill, J. H. *J. Mater. Sci.* **2001**, *36*, 3143–3164.
- (29) Yvon, K.; Jeitschko, W.; Parthé, E. *J. Appl. Crystallogr.* **1977**, *10*, 73–74.
- (30) Wesson, J. A.; Worcester, E. M.; Kleinman, J. G. *J. Urol.* **2000**, *163*, 1343–1348.

cure overnight. The embedded slices were ground flat, set in a 1 in. phenolic ring mount, flooded with petrooxy, and left to cure overnight. The samples were reflattened using a fixed 220 diamond grit lap wheel, followed by a 600 and a 1200 diamond grit. The samples were placed on a hot plate for 2 h to remove any moisture, at which time they were mounted on a glass slide and left overnight. The samples were removed from the hot plate and resectioned to a thickness of 300–500  $\mu\text{m}$  using a 100 grit circular diamond saw blade. The slices were ground down to 35  $\mu\text{m}$  using a 800 silicon carbide grit on a Logitech LP-30 optical grinding machine. Finally, the samples were transferred to a Whirlmet petro-thin machine and subjected to a three-stage, 15 min polishing using a cloth polish, followed by a diamond grit polish using 8000, then 11000, and finally 14000 grit. Polishing COM kidney stone samples has been demonstrated not to cause gross morphological changes.<sup>19</sup> Polished stone samples were examined using a polarizing microscope (Olympus BX60) and a Berek compensator.

**X-ray Diffraction (XRD).** X-ray diffraction was studied at room temperature using Reflection mode on a Rigaku R-AXIS rapid curved image plate detector with graphite monochromator, a Cu K $\alpha$  radiation source, a 0.3 mm collimator, and 25 min exposure. The reflected X-ray beam was measured from 5 to 80 degrees at 0.02 steps and 2 s per step. For XRD analysis, a suspension of powdered COM kidney stones was prepared by grinding stone samples using a standard laboratory mortar and pestle and then adding acetone directly to the mortar bowl. Using a Pasteur pipet, 4 to 5 drops of the resulting suspension were placed onto a square piece of a glass microscope slide (ca. 1  $\times$  1 cm) and heated in an oven at 60 °C for 5 min to evaporate the acetone and aid the sample sticking to the glass. COM crystals obtained from Fisher Scientific were mounted on a glass slide and analyzed on the XRD instrument under similar conditions.

### 3. Results

The main characteristics of the polycrystal morphology are the composition, size, shape, and orientation of constituting crystallites. The relevant information can be derived with the help of XRD and polarizing microscopy techniques, which we apply in the present work to study polycrystalline COM kidney stones.

COM has a monoclinic  $P2_1/c$  space group and the following crystal lattice parameters:  $a = 6.290 \text{ \AA}$ ,  $b = 14.583 \text{ \AA}$ ,  $c = 10.116 \text{ \AA}$ , and  $\beta = 109.46^\circ$ .<sup>31</sup> Monoclinic crystals are birefringent, having a refractive index that depends on the polarization direction of propagating light. This dependence can be characterized quantitatively with the help of optical indicatrix.<sup>32–34</sup> In crystals of a monoclinic system, optical indicatrix is represented by a triaxial ellipsoid. If the angles between the axes of indicatrix and the crystallographic axes are known, one can determine crystallographic directions from the optical data. To reveal these angles for COM structure, we studied the habits and optical properties of synthetic

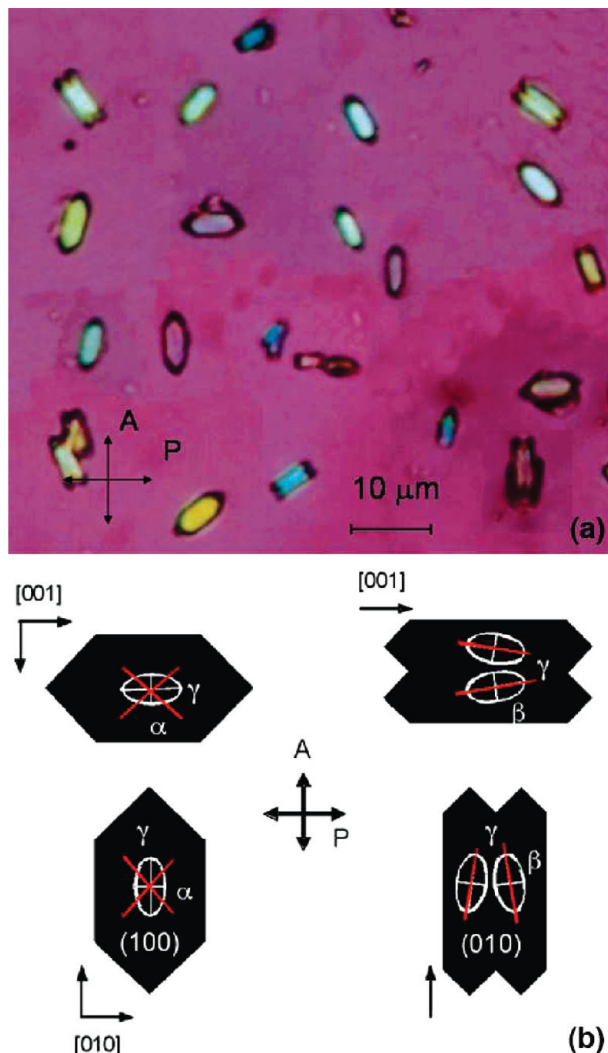


**Figure 1.** (a) Photograph of synthetic COM crystals between crossed polars with a superimposed first-order red plate, and (b) schematic representation of their morphology as seen under the microscope. Positions of polarizer (P), analyzer (A), and crystallographic axes are shown by arrows. The crystals in (a) which appear red (i.e., the same color as background) are in extinction positions. Crystals in (b) are shown in extinction positions (hexagonal crystals) or close to extinction positions (twins) with respect to the polars. Cross sections of optical indicatrix and optic axes are shown by white ellipses and red lines, respectively. Their positions in crystals are derived on the basis of observations and symmetry principles.

COM crystals. Cross sections of COM kidney stones are subsequently optically examined and regularities in the arrangement of crystallites are found. XRD data confirming the results of optical examination are also reported later.

**Examination of Synthetic COM Crystals.** Figure 1 shows COM crystals grown in our laboratory as described in the Experimental Procedures section. The morphology of crystals is in agreement with previous reports on synthetic COM crystals,<sup>23,35</sup> namely, one can observe two types of shapes: elongated hexagonal platelets and elongated contact twins with slightly split ends. The largest dimension can reach  $\sim 10 \mu\text{m}$ , and the

- (31) Tazzoli, V.; Domeneghetti, C. *Am. Mineral.* **1980**, 65, 327–334.
- (32) Wahlstrom, E. E. *Optical crystallography*. 5th ed.; John Wiley and Sons: New York, 1979.
- (33) Glazer, A. M.; Cox, K. G. In *International tables for crystallography*; Authier, A., Ed.; Physical properties of crystals, Vol. D; Academic Publishers: Dordrecht/Boston/London, 2003; p 522.
- (34) Nye, J. F. *Physical properties of crystals: their representation by tensors and matrices*; Clarendon Press: Oxford, 1964.

- (35) Cody, A. M.; Horner, H. T.; Cody, R. D. *Scanning Electron Microsc.* **1982**, Part I, 185–197.

thickness (measured by a Profilometer) is  $\sim 2 \mu\text{m}$ . The crystal habits are shown schematically in Figure 1b where faces and crystallographic directions are labeled in accordance with the literature.<sup>23,31,36</sup> Between the crossed polars, the crystals show white or pale-yellow first-order polarization colors.

The Neumann's Principle imposes specific limitations on the position of the optical indicatrix with respect to the symmetry elements of the crystal.<sup>34</sup> In particular, due to COM symmetry (point group 2/m), one of the axes of optical indicatrix ( $\alpha$ ,  $\beta$ , or  $\gamma$ ) should be parallel to the 2-fold symmetry axis, which is the [010] crystallographic axis, and the positions of the other two indicatrix axes are not restricted by symmetry. Therefore, the cross section of the indicatrix by the large face of hexagonal platelet, the (100) plane, is the ellipse with the axes parallel to [001] and [010] directions, respectively. This is shown in Figure 1b. When a transparent crystal plate is observed between the crossed polars, it should appear in extinction (i.e., become completely dark) when polarizer (or analyzer) is parallel to one of the axes of the ellipse.<sup>32,33</sup> In the left-hand part of Figure 1b, the two extinction positions of the (100) COM plate expected on the basis of the crystal symmetry are shown. In agreement with this theoretical expectation, we observed the extinction in hexagonal platelets when their elongation direction, the [001] crystallographic direction, coincided with the direction of the polarizer or analyzer. This is evident from photograph in Figure 1a. Note that this photograph is made with a first-order red plate inserted into the optical path. When this accessory plate is used, the crystal in extinction has characteristic first-order red color instead of being black. Nonbirefringent media (surrounding the crystal) has the same color (i.e., red with the first-order red plate and black without it). Therefore, without the first-order red plate, the black crystal in extinction would be undistinguishable on the black background.

As follows from the above discussion, the symmetry arguments do not help to determine the extinction positions, and therefore, the light vibration directions and indicatrix positions in (010) platelets (i.e., in COM twins which we observed). The experimental investigations are necessary. We observed that components of the twin cannot be positioned into complete extinction simultaneously. We found that one of the vibration directions deviate here by several degrees from the [001] direction (15° according to Hofmann)<sup>37</sup> and the deviation is opposite in different twin components as shown by the indicatrix ellipses in Figure 1b. This deviation is small and can be considered negligible in rough considerations.

We discriminate slow- and fast-ray vibration directions in the crystals (large and small axes of optical indicatrix, respectively) with the help of standard methods using a Berek compensator or the analysis of polarization colors in crystals with the superimposed first-order red plate. (Notice in Figure 1a the difference in colors of the crystals

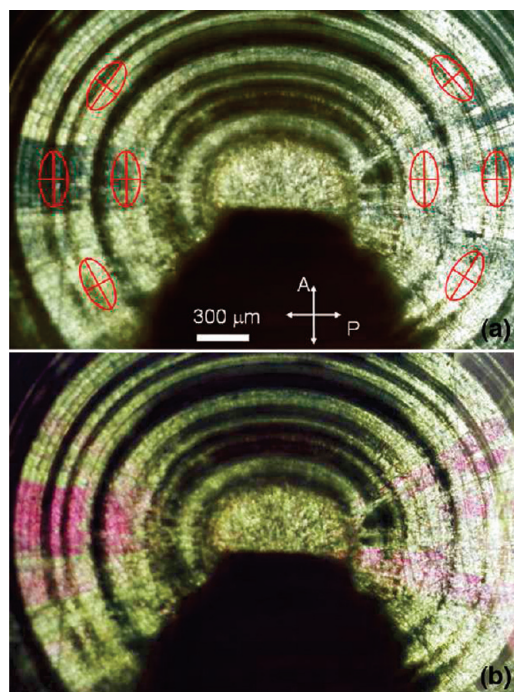


**Figure 2.** Competitively thick (0.2 mm) approximately diametric section of COM kidney stone viewed between crossed polars without (a) and with (b) the first-order red plate. Positions of the polarizer (P) and analyzer (A) are shown by arrows. Red-colored regions in (b) are the regions in extinction. Ellipses indicate the positions of optical indicatrix in different parts of the stone as determined from the extinction positions. The observed optical behavior is characteristic of spherulites.

rotated clock- and anticlockwise from the vertical position, respectively.) The optical indicatrix is found to be directed with respect to crystal habits as shown in Figure 1b. In other words, the axis of the indicatrix  $\gamma$ , which corresponds to the largest index of refraction  $n_\gamma$ , is directed approximately along [001]. We have no information available to determine the directions of optic axes and to distinguish two other indicatrix axis,  $\alpha$  and  $\beta$ ; however, the symmetry requirement is that the plane in which optic axes lie should be parallel or perpendicular to the [010] crystallographic axis. The former variant is shown in Figure 1b for definiteness. The angle between the optic axes is reported to be  $2V \approx 84^\circ$ .<sup>37</sup>

**Optical Investigation of Kidney Stones.** Using X-ray diffraction techniques, it is confirmed that the stones selected for optical examination have COM composition with crystalline impurities being absent. According to SEM data, the size of crystallites in COM kidney stones is  $\sim 0.1\text{--}1 \mu\text{m}$ .<sup>19</sup> Figure 2a shows the photograph of one of the samples between the crossed polars where the concentric laminar structure is evident, and extinction is observed in large areas. The view of the sample in the same position after insertion of a first-order red plate is shown in Figure 2b. This helps to distinguish between the regions that are really in extinction (they should become red in the presence of the first-order red plate) and opaque regions (which remain dark). Therefore, the concentric dark rings and the dark sector directed upward are the regions that do not transmit light (probably due to existence of foreign organic material between small-size

(36) Millan, A. *J. Mater. Sci.: Mater. Med.* **1997**, 8, 247–250.

(37) Hoffmann, W. *Naturwissenschaften* **1960**, 47, 38–39.

crystallites). On the contrary, the sectors directed to the left and to the right are the transparent regions in extinction. Note, however, that inside the dark (predominantly nontransparent) sector directed upward many small transparent red (i.e., in extinction) areas still exist. Therefore, the extinction pattern forms the cross. Such a kind of extinction is characteristic of spherulites<sup>39,40</sup> and has been already reported for COM kidney stones.<sup>26</sup> We observed some determinative features of spherulites, namely the extinction pattern, always had the shape of a Maltese cross with the arms parallel to the polarizer or analyzer (i.e., position of the cross did not change when the microscope table rotated). Optical behavior of spherulites is known to be related to their specific texture. With reference to our sample, the following interpretation can explain this behavior. The extinction should be observed if the vibration directions of the crystal coincide with the vibration directions of the polars. However, the thickness of the stone section we study is definitely much larger than the typical size of crystallites. In this case, the extinction can be observed only if all crystallites on the path of the light (from top to bottom of the specimen) have the same (or almost the same) vibration directions, which coincide with the vibration directions of the polars. Since the vibration directions are connected with the crystallographic orientation, our observation unambiguously suggests that crystallographic orientations of all crystallites from top to bottom of the sample are correlated (i.e., the crystallites are ordered). Furthermore, all the crystallites within the sectors that show simultaneous extinction have almost the same vibration directions and, therefore, ordered crystallographic directions. More precisely, a certain crystallographic direction in crystallites (we determine below that this is approximately the [100] direction) always remains parallel to the corresponding radial direction of the whole stone: only in this case, the observed crosslike extinction pattern is possible. We determined vibration directions in different parts of the stone as shown in Figure 2a. The spherical symmetry of the optical behavior that is characteristic of spherulites is evident.

Note that the regular extinction pattern is not observed in the core part of the stone section. Different crystallites demonstrate here the extinction at randomly different positions. In many regions all over the sample, the extinction cannot be observed at all, which means that the light propagates through two or more crystallites with different vibration directions, i.e., spherulitic ordering is not perfect.

For further investigations, we selected the thinner sections of stones with coarse microstructure (see Figures 3–6). When observed between the crossed polars, the specimens appear to be consisting of comparatively large regions (we call them “spherulitic domains” or simply “domains”) of different colors elongated approximately

(38) The color—retardation—thickness—birefringence relation is also represented by the Michel-Levy interference color chart.

(39) Morse, H. W.; Donnay, J. D. *Am. Mineral.* **1933**, *18*, 66–67.

(40) Keith, H. D.; Padden, F. J., Jr. *J. Appl. Phys.* **1964**, *35*, 1270–1285.

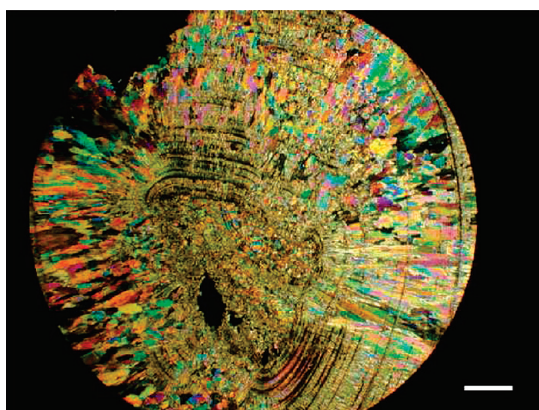


**Figure 3.** Thin (17  $\mu\text{m}$ ) approximately diametric section of COM kidney stone viewed between crossed polars. Scale bar is equal to 450  $\mu\text{m}$ . Spherulitic domains appear as regions of different color. Crystallographic axes of all crystallites within a domain are almost the same. That is why the color is homogeneous.

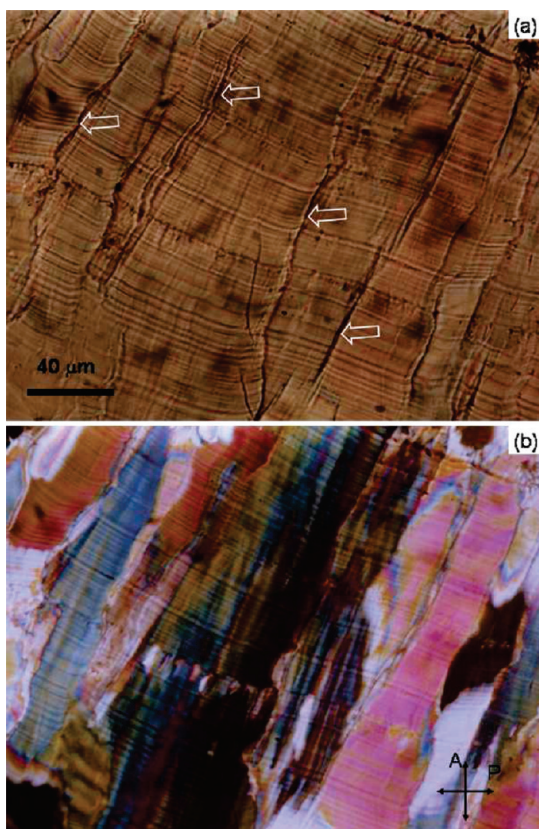


**Figure 4.** Fragment of the same specimen as in Figure 3 viewed in (a) plane-polarized light and (b) between crossed polars. The center of the stone is in the top-right direction. Arrows indicate domain boundaries. Segments of concentric dark rings approximately perpendicular to domain boundaries are presumably the organic layers.

along the corresponding radial direction of the specimen. The largest dimension of domains is typically 50–400  $\mu\text{m}$ , but many smaller domains and several larger ones can be found. In the core region of the stone section, the domains are comparatively small and have equilateral rather than elongated shape (Figure 6a).

Every domain appears to be in extinction (becomes completely dark) at certain positions of crossed polars, which can be significantly different in neighboring domains

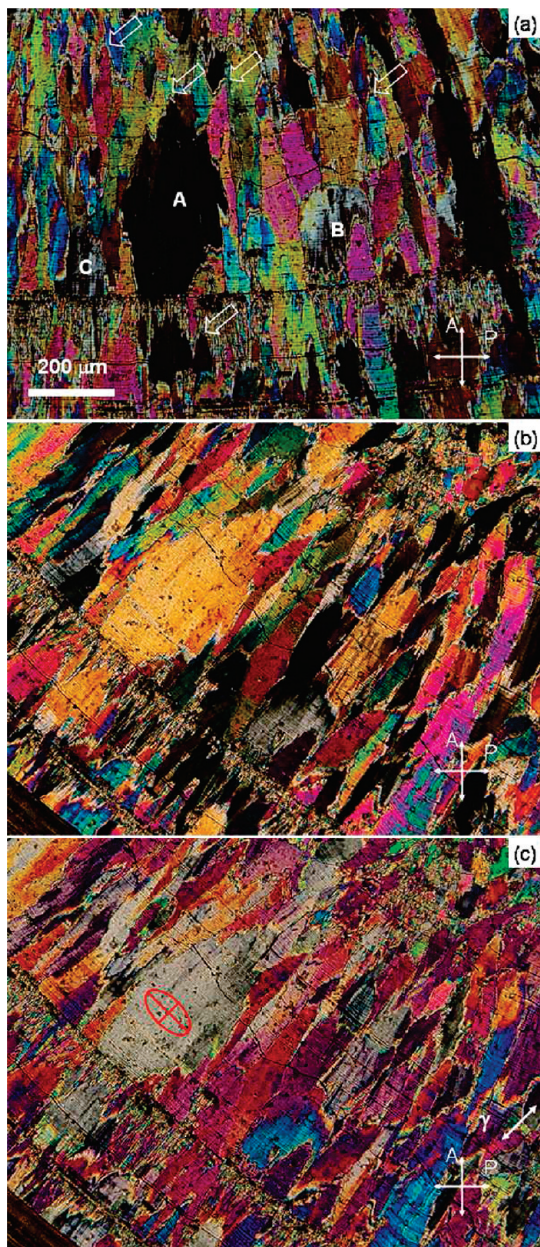


**Figure 5.** Fragment of the same specimen as in Figure 3 viewed in crossed polars at different positions of the microscope rotating stage to establish the fast and slow vibration directions in domain A. (a) Domain A and some other domains are in extinction (black). The center of the stone is on the top. (b) Domain A is in a diagonal position; some other domains are in extinction. (c) Same view as (b) but with an inserted first-order red accessory plate. The positions of polarizers and the slow vibration direction  $\gamma$  of the accessory plate are shown by arrows. The determined position of indicatrix in the domain A is shown by red ellipse in (c). Thick arrows in (a) indicate the points from which the domains start growing.

(compare Figure 5a,b). The colors of domains are obviously the polarization colors that should emerge in birefringent sections of certain thickness under the crossed polars. The polarization colors are known to be determined by the retardation,  $R$  (path difference between propagating slow and fast waves), and depend on the thickness of the observed specimen ( $h$ ) and the birefringence of the material in the direction of light propagation ( $\Delta n$ ) according to the following relation:<sup>38</sup>

$$R = h\Delta n \quad (1)$$

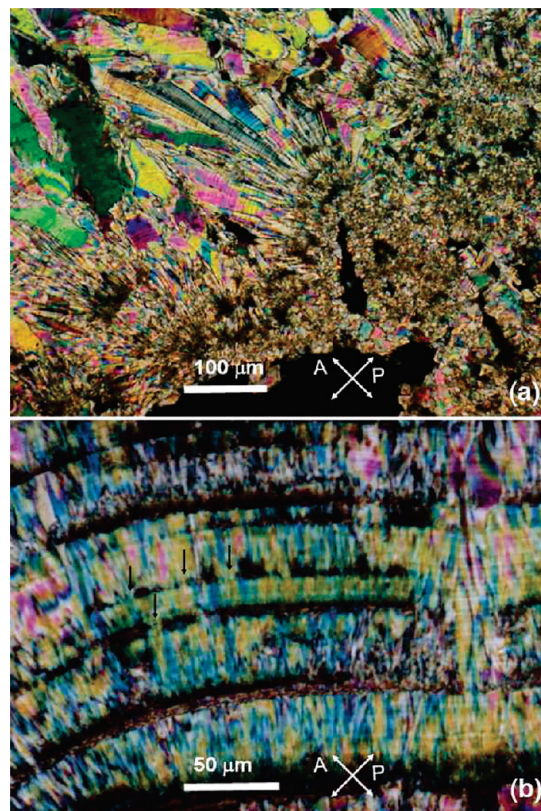


**Figure 6.** Fragments of the same specimen as in Figure 3. (a) The domains in the central region of the stone (the bottom-right part of the figure) are nearly equilateral in contrast to elongated domains in other regions. (b) Areas of the same color (i.e., the same crystal orientation) propagate through dark organic layers. The black arrows indicate growth channels.

Birefringence, in its turn, depends on crystallographic direction. As the thickness of the specimen is constant, the homogeneous color of the domain unambiguously suggests that all crystallites inside the domain have the same crystallographic orientation. This is further confirmed by the fact that every domain can be put into complete extinction. Accordingly, different colors in different domains out of the core region of the stone section, the colors are of the third or lower order. The largest retardation measured in these domains with a Berek compensator is 1670 nm which corresponds to the birefringence value of 0.098. In contrast, the core domains often demonstrate pale fourth- and fifth-order colors. This difference is seen in Figure 6a, in which the core area (in the right-hand part) and the remote areas are shown.

On the smaller length-scale, every domain consists of bright concentric layers 0.5–3  $\mu\text{m}$  thick separated by dark boundaries; the thickness of which is usually much smaller than 1  $\mu\text{m}$  and cannot be resolved even under the largest microscope magnification. The concentric boundaries are clearly visible even without the analyzer (i.e., in plane-polarized light) (see Figure 4a). Each boundary often spreads without termination through many domains which suggests that each concentric layer appears simultaneously in different domains in the course of growth process. Domains of different color are also often

(but not always) separated by thin black boundaries. The black boundaries may have different (probably organic) composition. On the other hand, in the plain-polarized light, one cannot resolve any radial striation within the majority of the domain. In some domains, the radial lines are visible, but they are wavy and much less prominent than the concentric ones. The prominent radial structure inside the domain may appear only between crossed polars in the form of "rays" having slightly different polarization colors and/or slightly different extinction positions (Figure 4b). This suggests that radial structure is related to the slightly different orientation of neighboring crystallites rather than to the existence of the material boundaries (e.g., organic) between them.

As the macroscopic symmetry of the spherulite (in particular, the symmetry of optical properties) is spherical, one needs to distinguish two types of directions: radial direction, which is thought to coincide (at least approximately) with the direction of kidney stone growth, and the directions perpendicular to the radius. In every point of the sample, all the directions perpendicular to the radius are equivalent. There also must be certain relation between macroscopic directions and the crystallographic directions of the constituent crystallites. In particular, one can immediately conclude that the [001] crystallographic direction (which is approximately the same as the direction of the largest axis of optical indicatrix  $\gamma$ , according to Figure 1b) should be perpendicular (as in Figure 2a) or parallel to the radial direction (otherwise the extinctions shown in Figure 2 would be impossible). To elucidate which of these options is realized, we determined the slow and fast vibration directions in different domains. It was found that in the majority of domains the slow vibration direction is approximately perpendicular to the radial direction. Figure 5 illustrates this behavior for one of the domains labeled by letter A. Being in diagonal position (Figure 5b), it shows first-order yellow color. (Measurement with the Berek compensator gives the value of  $R = 380$  nm in the domain center.) With the first-order red accessory plate in case of subtraction, the retardation should be  $R = 530 - 380 = 150$  nm, which corresponds to the gray color. This color is really observed when radial direction of the domain is parallel to the slow direction of accessory plate (Figure 5c). This means that slow vibration direction of the domain A is perpendicular to the radial direction and excludes the possibility of parallelism between the radial direction and [001].

There is another way to show that  $\gamma$  and [001] are perpendicular to the radial direction of the stone. If this is not so (i.e.,  $\gamma$  is along the radius of the stone), then the variation of retardation (polarization colors) in a different domain is due to the rotation of the two other axes of indicatrix,  $\alpha$  and  $\beta$  in the plane, perpendicular to the radius. Using eq 1, the known sample thickness  $h = 17 \mu\text{m}$  and the values of  $n_\alpha = 1.491$ ,  $n_\beta = 1.556$ , and  $n_\gamma = 1.650$  for COM,<sup>37</sup> we can calculate that  $R$  may vary in this case from  $h(n_\gamma - n_\alpha) \approx 2700$  nm (when  $\beta$  axis is along the viewing direction) to  $h(n_\gamma - n_\beta) \approx 1600$  nm (when  $\alpha$  axis is

along the viewing direction). This retardation interval corresponds to the fourth- and fifth-order polarization colors which were not observed in the domains not belonging to the core. Therefore, this configuration is nonexistent. On the other hand, this stone section does not contain the very "center" of the stone from which the growth process started. Therefore, radial direction of the whole stone and radial direction of the studied section are not always the same. In the core region of the section, the radial direction of the stone is parallel (or almost parallel) to the viewing direction. In this case,  $\gamma$  perpendicular to the radius of the stone should be in the plane of the section and, as discussed above, should give rise to the retardation between 1600 and 2700 nm (fourth- and fifth-order polarization colors). This is easily apparent in Figure 6a, which shows the central region of the stone (in the bottom-right part of the figure).

Therefore, the data can be explained by the suggestion that  $\beta$  axis of indicatrix, which is approximately perpendicular to (100), according to Figure 1b, is along the radial direction in all domains and the directions of  $\alpha$  and  $\gamma$  may vary in the perpendicular plane giving rise to different polarization colors in different domains. If one of the optic axes (which are in the  $\alpha-\gamma$  plane) accidentally becomes parallel to the viewing direction, the domain remains in extinction in any position with respect to the polars. A few domains of such a kind were observed (e.g., domains B and C in Figure 5).

Many domains (some of them are shown by arrows in Figure 5a) are sharpened in the direction of the stone center. This implies the conical shape of domains at least in the early stages of their growth, such as the apex of the cone is the starting point of the growth. In the advanced growth stages, the neighboring domains interact and their shape may change (become nearly cylindrical). Note that the apex itself can be seen only if it lies exactly in the studied stone plate, otherwise the domain shape should be represented by conic sections (hyperbolas or parabolas). This is really the case for many domains (e.g., domain B in Figure 5a). In the core of the specimen where the growing direction is approximately along the viewing direction, the conic section should be represented by ellipse or circle. This explains equilateral shape of core domains that are in fact the circles damaged by interactions with the neighboring domains.

**X-ray Diffraction Investigation of Kidney Stones.** To study further the texture in kidney stone specimens, their XRD patterns were compared with the patterns of COM powder and diffraction profiles calculated by means of the computer program LAZY PULVERIX<sup>29</sup> using the known structural parameters for COM.<sup>31</sup> Figure 7 shows the part of the XRD spectrum obtained from the surface of the diametric section of one of the specimens. Comparison with theoretical pattern reveals no additional diffraction peaks, which would signify crystalline impurities in the stone. However, the intensities of all (h00) peaks are found to be dramatically reduced as compared to calculated and powder profiles. This feature strongly suggests the existence of a texture (i.e., preferred

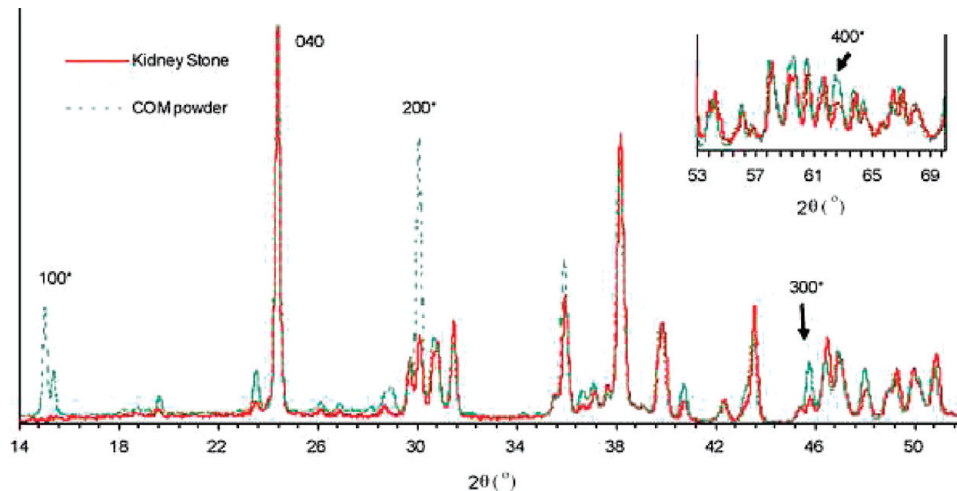


**Figure 7.** X-ray diffraction pattern of commercial COM powder and the diametric section of kidney stone. Intensities are normalized to obtained equal values for the most prominent (040) peak. Diffraction peaks missing in the stone are marked by an asterisk. Missing peaks indicate the presence of preferable directions in the arrangement of crystallites (texture).

crystallographic orientation of crystallites within the polycrystalline specimen). The (h00) peaks appear due to interference between the waves reflected from (100) crystal planes. The absence of these peaks means the absence of crystallites in which (100) planes are parallel to the surface of the studied specimen. Such a kind of texture is consistent with the spherulitic crystallites arrangement derived from optical observations, which require the (100) planes to be perpendicular to the radial direction of the stone and, consequently, perpendicular to diametric cross sections. XRD data confirm, therefore, the results of polarizing microscopy.

Note that the effect of (h00) peak suppression can be different in the different areas of the same stone section and are not observed in all studied stones. This can be explained by the features of experimental technique. The X-ray beam in the XRD experiment samples a comparatively large area ( $\sim 0.5$  mm). If the size of spherulitic domains is much smaller, and their radial directions are not ordered along the radial direction of the stone, they are seen by XRD as disordered crystallites and the texture cannot be revealed. Polarizing microscopy works on a much smaller scale and even tiny ( $\sim 10$   $\mu\text{m}$ ) spherulitic domains can be distinguished as arrays of different colors.

#### 4. Discussion

Our results show that the crystallographic orientations of crystallites that compose a kidney stone are not random. Within comparatively large, dozens and hundreds of micrometer domains, all crystallites retain, almost perfectly, the same crystallographic orientation. In some stones, such as those depicted in Figure 3, this nearly perfect order is violated on a larger scale (i.e., the directions of different domains are different). In other cases (Figure 2), the correlation length of ordering appears to be much larger, vibration directions (and, therefore, related crystallographic features) are aligned along radial directions in the whole sample. However, in any case, the

crystallites located in different regions of the stone are not independent units. They are parts of a coherent network where every crystallite “knows” the orientation of other ones in the remote location. This network cannot be formed by means of occasional trapping of already existing microcrystals from urine as suggested by some model of kidney stone growth.<sup>18,19</sup> Such trapping implies that the orientations of joining microcrystals and, consequently, the orientation of crystallites within the stone should be random.<sup>18,19</sup> The observed ordering strongly suggests the essential role of the direct crystal-growth mechanism of kidney stone formation. The hypothesis that spherulitic domains may grow separately and then aggregate to form the stone should also be rejected as nonrealistic. Their large size, orientation (apex directed preferably to the center of the stone), complex shape, and thin ( $< 1 \mu\text{m}$ ) boundaries between them suggest that they grow together. The boundaries are evidently formed in the course of interactions between growing domains.

**COM versus Normal Spherulitic Growth.** Despite apparent differences in the morphology of stones shown in Figures 2 and 3, we suppose that the growth mechanism is basically the same in both cases and differences are due to some variations of growth conditions. Examination of Figure 2 shows the extinction characteristic of spherulites. Therefore, the natural step of the discussion should be the comparison of our data with those inherent in typical spherulites. As follows from our observations, kidney stones are distinguished by at least four significant features. These differences are depicted schematically in Figure 8.

Spherulites usually consist of crystalline fibers radiating from a common center, the nucleus from which fibers begin to grow.<sup>27,39,40</sup> Lateral dimensions of growing fibers remain remarkably constant and filling of the space by crystalline material occurs via numerous branching of fibers, as shown schematically in Figure 8a. This branching is noncrystallographic, in contrast to dendritic branching (i.e., crystallographic orientation in daughter fibers differ from the orientation of parent fiber). The

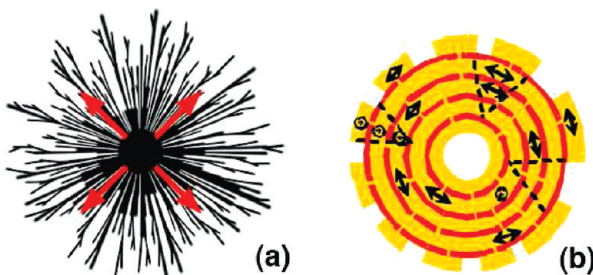


**Figure 8.** Schematics of (a) the radial morphology of a normal spherulite and (b) layered morphology of a kidney stone. Arrows show the fast-growing directions of crystallites. Crystalline and amorphous material in (b) are shown by yellow and red color, respectively. Some of the spherulitic domains are shown by broken lines.

difference is generally small, and because of this, certain crystallographic direction remains almost parallel to the radial direction giving rise to the characteristic crosslike extinction pattern under the polarizing microscope. Impurities and noncrystalline substances accumulate between the fibers increasing their visibility. The first unusual feature of kidney stones is that the prominent radiating fiber structure is absent (Figures 2 and 4a). SEM images of COM stones subjected to proteolysis also reveal a platelike rather than fiberlike shape of COM crystallites.<sup>18,19</sup>

The comprehensive phenomenological model of Keith and Padden<sup>27</sup> attributes the branching in spherulites to heterogeneities such as impurities or molecular defects which perturb crystallization by deflecting the tips of growing fibers. While different reasons for noncrystallographic branching were also proposed,<sup>41</sup> the common feature of existing models of spherulitic growth is that the fast growth direction in any point of growth front is approximately parallel to the radius of the spherulite. This feature also appears in computer simulations in the mainframe of the generalized phase field model of polycrystalline growth.<sup>41,42</sup>

As follows from our observations of synthetic crystals, [001] is the fast growth direction for COM. A. Millan performed elaborate theoretical calculations and experiments on COM crystal growth under different conditions, analyzed COM crystal morphology encountered in nature, and came to the conclusion that this is the general rule.<sup>23</sup> More specifically, early crystals are needlelike and elongated along the [001] direction. With growing time, they become tabular, but the size along [001] remains the largest one. On the basis of this information, it was proposed that radially oriented needlelike (fiber) COM crystallites may form the structure typical of spherulites.<sup>23</sup> However, our observations unambiguously show that the [001] (i.e., fast growth) direction is perpendicular to the radius instead of being radial.

The third important feature of kidney stones that is absent in most spherulites is the concentric layered structure, which is suggested to be related to the irregular

distribution of pigment (similar to some mineral spherulites).<sup>26</sup> Our observations rather indicate the existence of thin opaque layers of different composition.

Finally, COM stones may contain domains in which the crystallographic axis of crystallites has almost the same direction, while in the neighboring domains the direction is significantly different.

**Proposed Model of COM Kidney Stone Growth.** To account for the mentioned features of kidney stone morphology, we propose the following model of growth by considering the layered characteristic in details. Figure 9 shows schematically how it may happen starting from the initial microcrystal appearing for some reason (which will be discussed later) on the surface of the stone. Similar to other crystallites, the (100) plane of this microcrystal is perpendicular to the radial direction of the stone, as shown in Figure 9a. We use the known fact that kidney stones always contain organic matrix (proteins, lipids, polysaccharides etc.) embedded between the crystallites.<sup>2,18,43</sup> The presence of organic components in urine may inhibit the growth of crystallites.<sup>18,44–46</sup> Layered morphology observed under the microscope is supposed to be related to the periodic variation of growth conditions. In the time intervals when the role of inhibitors is comparatively small, crystallites grow freely. During the time interval when for some reasons the crystal growth rate decreases or the rate of precipitation of organic molecules on the surface increases, the crystal layer appears to be covered significantly by the organic material (Figure 9b). Remaining spots free from the organic matrix serve as “seeds” for further crystallization. Crystallites grown around these spots in the next stage of the process should have the same orientation as a parent crystallite (Figure 9c). These new crystallites grow until they coalesce and fill all the space between them. Note that the direction perpendicular to (100) is the slowest growth direction; thus, a thin crystal layer is formed as a result of coalescence. At the next stage, the rate of organic matrix deposition again increases (or crystal growth rate decreases) and the next opaque organic layer appears. Then, the process is repeated.

As a result of this process, the crystal layers are formed, which are separated by organic interlayers. However, the organic interlayers are not continuous. The crystal structure grows through “channels” which connect neighboring crystal layers. Though these channels are supposed to have submicrometer size, they can sometimes be observed on a larger scale, as one can see in Figure 6b, where the areas of the same color (i.e., the same crystal orientation) propagate through dark organic layers. Due to these growth channels, the same crystallographic orientation is maintained throughout the spherulitic domain. In this

- (41) Gránásy, L.; Pusztaí, G.; Tegze, G.; Warren, J. A.; Douglas, J. F. *Phys. Rev. E* **2005**, 72, 011605.  
 (42) Gránásy, L.; Pusztaí, G.; Borzsonyi, T.; Warren, J. A.; Douglas, J. F. *Nat. Mater.* **2004**, 3, 645–650.

- (43) Khan, S. R.; Glenton, P. A.; Backov, R.; Talham, D. R. *Kidney Int.* **2002**, 62, 2062–2072.  
 (44) Jung, T.; Sheng, X.; Choi, C. K.; Kim, W. S.; Wesson, J. A.; Ward, M. D. *Langmuir* **2004**, 20, 8587–8596.  
 (45) Wesson, J. A.; Ganne, V.; Beshensky, A. M.; Kleinman, J. G. *Urol. Res.* **2005**, 33, 206–212.  
 (46) Ryall, R. L.; Fleming, D. E.; Grover, P. K.; Chauvet, M.; Dean, C. J.; Marshall, V. R. *Mol. Urol.* **2000**, 4, 391–402.

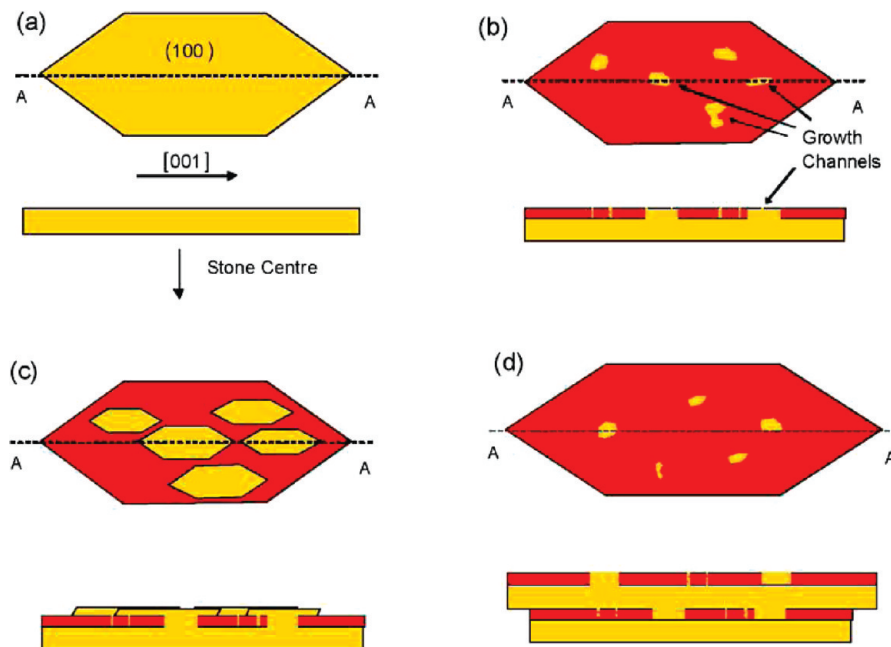


**Figure 9.** Schematics of a periodic growth process leading to layered morphology. (a–d) Sequential stages of the process; top view and the cross section along A–A line. Crystalline and organic materials are shown by yellow and red color, respectively.

idealized interpretation, the process is similar to the dendritic crystallization rather than to spherulitic growth. In particular, it should lead to the formation of flat layers. In reality, the layers are often slightly curved (see Figure 4) presumably due to the noncrystallographic small-angle branching, similar to “normal” spherulites. However, this branching occurs in the radial direction (i.e., direction perpendicular to the fast-growth [001] direction). As discussed above in this section, the impurities, in particular the organic molecules, may cause the branching.

Consider now the developments of the spherulitic domain, which arises from the initial “seed” crystallite and develops into a nearly conic shape. The crystallographic directions in different domains are found to be different. The direction in every domain must be determined by the position of the seed crystal located at the apex of the growing cone. On the other hand, we did not observe the relation between the crystallographic orientation of the newborn and already existing domains, except the requirements that the (100) crystallographic plane should be approximately perpendicular to the domain radial direction (parallel to the organic layers). Therefore, the seed crystal is not connected by the growth channels with the previous crystal layer. The possible ways for such a kind of seed crystal to appear is the deposition of the existing microcrystal from urine on the organic layer as shown schematically in Figure 10a. Since the most prominent (100) face of COM crystals is also the most adhesive one,<sup>18</sup> the requirement that the (100) plane of seed crystal be parallel to the organic layer can be satisfied. The absorbed microcrystal creates a hump on the surface of the stone (Figure 10b), which limits the growth of the next crystal layer of the old domain (Figure 10c). At the same time, the growth of the next

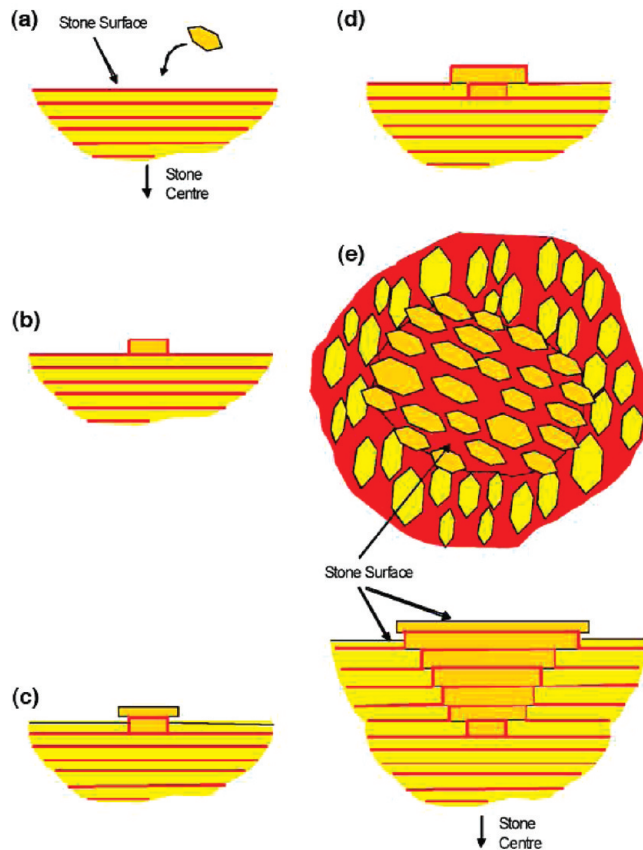


**Figure 10.** Growth of new domain on the free surface of existing domain. (a–e) Sequential stages of the process; diametric cross section of the stone is shown, and in (e), the top view is also shown. Organic matrix is represented by the red color, crystalline material of “newborn” and “old” domains are dark-yellow and light-yellow, respectively. Growth channels between crystalline layers are not shown. The growth of the last crystal layer is not completed.

crystal layer of the newborn domain is not limited and it can expand in lateral directions. The newborn domain is

high at all subsequent growth stages (Figure 10d,e) so that it becomes wider during growth until it meets with similar neighboring domain.

The surface of the stone may not be ideally even so that the (100) plane of the deposited seed microcrystal and, consequently, the (100) plane of the whole newborn domain may not be perpendicular to the corresponding radial direction of the stone. Therefore, the roughness of the stone surface leads to the additional disorder in the mutual arrangement of domains grown on this surface. This explains why the neighboring domains may have very different extinction positions under the polarizing microscope (e.g., in Figure 5). In some specimens, this kind of disorder is small, extinction positions of neighboring domains are close and characteristic spherulitic extinction pattern (cross) can be observed (see Figure 2).

The size of spherulitic domains is determined by the rate of preformed microcrystal adhesion as compared to the rate of crystallization. If the former is comparatively large, the size of the domains is small as, for example, in the stone shown in Figure 2 or in the lower part of the stone in Figure 5 (a). The role of microcrystal adhesion is also critical for the formation of large-size stones. If the direct crystal growth is terminated due to precipitation of an unusually large amount of organic material on the stone's surface, microcrystals deposited from urine can give rise to the formation of new domains, thus maintaining the further growth of the stone. This can explain, in particular, why calcium oxalate dihydrate (COD) is rarely observed in kidney stones in spite of the large concentration of COD microcrystals in urine. Adhesion force for COD is measured to be considerably smaller than for COM, and thus, the mechanism of the attachment of COD microcrystals is not effective.<sup>18</sup> Moreover, new domains are not expected to appear when COD crystallization is terminated by organic matrix.

It is clear that the considered mechanism leads to the conservation of the shape of growing stone, i.e., a well-developed sphere should remain a sphere, at least approximately. The behavior in the initial steps of stone formation starting from the "first" seed crystal is not so evident. The morphology of the core and the surrounding parts in the stone sections we studied (see Figures 2, 3 and 6a) is different. As discussed in the previous section, this can be attributed to the fact that the stone sections are not exactly diametric. However, other different mechanisms of core formation cannot be excluded. Unfortunately, we have no experimental data to draw definite conclusions. To perform observations, one needs to study the cross section which contains the very "center" of the stone. However, it is difficult to prepare such a section due to lack of a priori information about its position.

The derived model based on the polarized light microscopy and XRD investigations is consistent with the results of scanning electron microscopy (SEM) and atomic force microscopy of kidney stones that provide images with much larger magnification. These techniques clearly revealed the COM crystals in the form of

plates stacked on their large (100) faces,<sup>19</sup> in agreement with our results. The crystalline channels (or "bridges"), through an organic matrix similar to those we postulated to explain the coherence of a crystal structure in different spherulitic layers, had been observed between crystallites in nacre<sup>47</sup> and other biominerals.<sup>48</sup> However, the channels in spherulites have not been reported so far.

## 5. Conclusions

In the present work, we studied COM kidney stones and determined that the continuous crystallization (monoepitaxial growth) mechanism is definitely involved in their formation. To explain the stone morphology, we proposed the model suggesting that the continuous crystallization and aggregation via adhesion of preformed microcrystals from urine, which were considered so far as two alternative mechanisms of kidney stone formation, are actually both important. Crystallization is the primary way for the development of comparatively large (up to ~0.5 mm) and independent polycrystal blocks (domains) which constitute the COM stone. Preformed microcrystals are considered to be responsible for the appearance of new spherulitic domains. Being deposited on the surface of the growing domain, they disrupt the preferred orientation of crystallites and serve as seeds for crystallization of new domains with different crystallographic orientations.

The role of organic matrix is considered to be crucial. In particular, precipitation of organic molecules seems to be responsible for the noncrystallographic small-angle branching of growing crystals (a common feature of spherulite formation) giving rise to the spherical shape of layers inside the domains. Periodic increasing of the precipitation rate with respect to the crystallization rate inhibits further crystallization and leads to the formation of a layered structure. Besides, the organic matrix promotes the formation of new spherulitic domains by means of occasional trapping of preformed microcrystals from urine. Although the proposed model of stone development does not consider heteroepitaxial growth, it may be active under certain conditions, thus complicating the process. Further, investigations are needed to clarify the initial stages of stone formation.

While COM kidney stones demonstrate the main spherulitic feature, namely the ordering of a certain crystallographic direction of crystallites along the corresponding radial direction of the specimen, substantial distinctions from known so far spherulites are found, namely the morphology of concentric spherical layers and perpendicular orientation of COM fast growing direction to the corresponding radial direction of the spherulite. This distinction is suggested to be a result of specific

(47) Schaffer, T. E.; Ionescu-Zanetti, C.; Proksch, R.; Fritz, M.; Walters, D. A.; Almqvist, N.; Zaremba, C. M.; Belcher, A. M.; Smith, B. L.; Stucky, G. D.; Morse, D. E.; Hansma, P. K. *Chem. Mater.* **1997**, *9*, 1731–1740.

(48) Imai, H.; Oaki, Y.; Kotachi, A. *Bull. Chem. Soc. Jpn.* **2006**, *79*, 1834–1851.

growth conditions, in particular, their periodicity, which is evidently related to the biological cycles in the human body.

**Acknowledgment.** This work was supported by the Natural Sciences and Engineering Research Council of Canada

(NSERC), the Canada Research Chair Program and Simon Fraser University (through the SFU Community Trust Endowment Fund), and generous grants from the Department of Chemistry and the Department of Graduate Studies at Simon Fraser University to U.A.-A.